Available online at www.sciencedirect.com
SCIENCE DIRECT®
Journal of Chromatography A, 1079 (2005) 299–306
JOURNAL OF CHROMATOGRAPHY A
www.elsevier.com/locate/chroma

Use of electrokinetic measurements for characterization of columns used in capillary electrochromatography

Anurag S. Rathore [a,*], Yan Li [b], James Wilkins [b]

[a] *Amgen Inc., Mail Stop 30W-2-A, 1 Amgen Center Drive, Thousand Oaks, CA 91320, USA*
[b] *Yale University, New Haven, CT 06511, USA*

Available online 7 April 2005

Abstract

The separation mechanism in capillary electrochromatography (CEC) is a hybrid differential migration process, which entails the features of both high-performance liquid chromatography (HPLC) and capillary zone electrophoresis (CZE), i.e., chromatographic retention and electrophoretic migration. The focus of this paper is on the use of electrokinetic data, such as current, electroosmotic flow (EOF) and column efficiency measurements, that are readily available, for an improved understanding of CEC separations. A framework is presented here for the use of this data for evaluation of a variety of performance parameters including, conductivity ratio, interstitial EOF mobility, porosity, and zeta potential. This framework is applied for characterization of two monolithic columns with different chemistry that were manufactured in-house. The above-mentioned performance parameters were calculated for the two columns and it is found that the poly(VBC–EGDMA–SWNT) monolithic column with the GPTMS–PEI coating offers a significantly improved flow distribution in comparison to the poly(VBC–EGDMA) monolithic column. This observation is confirmed by performing separation of peptides on the two columns and height equivalent of a theoretical plate (HETP) measurements on the resulting peaks. It is shown that following our approach leads to an improved understanding of the separations achieved with the columns and to better column design.

Keywords: CEC; Electrochromatography; Characterization; Monolith columns; Conductivity; Mobility; HETP

1. Introduction

Capillary electrochromatography (CEC) is an analytical separation technique that is carried out most commonly with packed capillary columns and utilizes electroosmotically driven mobile phase at high electric field strength in an apparatus similar to that used in capillary zone electrophoresis (CZE). Recently, CEC has attracted considerable interest due to its potential to offer high resolution and different selectivity than in HPLC and CZE [1–16].

The focus of this paper is on the use of electrokinetic data, such as current, electroosmotic flow (EOF) and column efficiency measurements, that are readily available, for an improved understanding of CEC separations. We use the framework that we have previously published [12,17] for evaluation of a variety of performance parameters commonly used for characterization of CEC columns. The results show that estimation of these performance parameters lead to an improved understanding of the separations achieved with the columns and can assist in column design.

2. Theory

2.1. Measurement of current

In this section, we present a discussion of the equations that have been used for data analysis. A more detailed description of the framework used was published earlier [12,17].

In an open capillary, when ionic conduction through the bulk electrolyte is the dominant mechanism of ionic migration, the conductivity of an electrolyte, σ_{open}, is expressed as

$$\sigma_{\text{open}} = \frac{iL_{\text{open}}}{V_{\text{open}}A_{\text{open}}} \quad (1)$$

where i is the current flowing through a capillary of length L_{open} and cross-sectional area A_{open}, when a potential drop V_{open} is applied across it.

* Corresponding author. Tel.: +1 805 447 4491; fax: +1 805 499 5008.
E-mail address: arathore@amgen.com (A.S. Rathore).

0021-9673/$ – see front matter © 2005 Elsevier B.V. All rights reserved.
doi:10.1016/j.chroma.2005.03.050

Eq. (1) can be extended to the case of a packed column or monolith when ionic conduction through the bulk electrolyte solution is still the primary form of ionic migration. Conductivity of the packed column, σ_{packed}, can then be expressed in the following manner

$$\sigma_{packed} = \frac{i' L_{packed}}{V_{packed} A_{open}} \quad (2)$$

where i' is the current flowing through the CEC column fully packed with a stationary phase. L_{packed} is the length of the column and V_{packed} is the applied voltage.

If measured under identical conditions of the mobile phase, the ratio of the conductivities of a packed column and open capillary, ϕ, has been known to have been a useful means for characterizing the properties of the stationary phase [12,17–19]. The conductivity ratio is related to the electrokinetic porosity, ε_T, by Archie's law as follows

$$\phi = \frac{\sigma_{packed}}{\sigma_{open}} = \varepsilon_T^m \quad (3)$$

where ε_T is the electrokinetic porosity and m is an empirical constant. When the porosity of the media is greater than 0.2, $m = 1.5$ provides a very close approximation to the experimental data [12,17–19] and so this value has been used for our calculations.

2.2. Measurement of flow

In open tubes with thin double layers and when there is no polarization, the EOF mobility, $\mu_{eo,open}$, can be expressed by the following relationship introduced by von Smoluchowski [20,21]

$$\mu_{eo,open} = \frac{\varepsilon \varepsilon_0 \zeta_w}{\eta} \quad (4)$$

where ε is the dielectric constant of the medium, ε_0 is the permittivity of the vacuum, and η is the viscosity of the bulk solution and ζ_w is the zeta potential at the capillary inner wall. For a fully packed column, EOF mobility in the interstices, $\mu_{eo,packed}$, can been expressed in a similar manner [17,20,22]

$$\mu_{eo,packed} = \frac{\varepsilon \varepsilon_0 \zeta_s}{\eta} \quad (5)$$

where ζ_s is the zeta potential at the surface of the packing.

In practice, the EOF mobility in the bulk electrolyte is estimated from migration data obtained with a suitable neutral and inert tracer in an open tube by using the following expression

$$\mu_{eo,open} = \frac{L_d L_{open}}{t_{0,open} V_{open}} \quad (6)$$

where L_d is the distance between the inlet and the point of detection of the capillary and $t_{0,open}$ is the migration time of the tracer in an open tube. The corresponding expression for a fully packed column would be as follows

$$\mu^*_{eo,packed} = \frac{L_d L_{packed}}{t_{0,packed} V_{packed}} \quad (7)$$

where $t_{0,packed}$ is the migration time of the inert tracer in the column. However, the mobility, $\mu^*_{eo,packed}$, calculated in this manner is the "apparent" EOF mobility [12,17] as unlike the mobility for open tube, the apparent EOF mobility would depend on the porosity and architecture of the packing, as they determine the path the ions need to take while flowing through the column. The actual interstitial mobility of an inert, neutral EOF marker through the packed segment that would be useful for determining the zeta potential of the packing should be calculated as [12,17]

$$\mu_{eo,packed} = \frac{L_e^2}{t_{0,packed} V_{packed}} \quad (8)$$

where L_e is defined as the length of the actual flow path followed by the tracer traversing a packed column of length L_{packed}. It can be calculated from the currents in the open and packed columns as follows

$$L_e = L_{packed} \sqrt{\frac{i_{open}}{i_{packed}}} \quad (9)$$

It must be reiterated that the effect of tortuosity has to be taken into account so that $\mu_{eo,packed}$ can be used to provide an accurate estimation of the zeta potential of the packing [12,17].

2.3. Measurement of column efficiency

This section deals with the column efficiency measurements as performed with a neutral and inert (non-interacting) tracer. The height equivalent of a theoretical plate (HETP) is commonly used as a measure of column efficiency and is expressed by the van Deemter equation as follows [23]

$$\text{HETP} = H_A + H_B + H_C \quad (10)$$

where H_A, H_B and H_C are the three major contributions to band broadening. The "A" term represents the contribution to the plate height from flow maldistribution in the packed column in the absence of extra-column effects. It is also referred to as the "eddy diffusion" term [24]. The B term stands for band spreading resulting from longitudinal diffusion of the sample component and contributes significantly to the plate height only at low flow velocities. As in traditional HPLC, this term is negligibly small for common CEC operating conditions. The C term arises from mass transfer resistances encountered by the sample components in the retention process based on their distribution between the mobile and stationary phases [24]. For columns packed with porous stationary phase particles, the C parameter is largely determined by kinetics of both the intraparticular mass transfer and film diffusion.

For the case of an open capillary and in absence of Joule heating, the velocity profile is approximately flat for electrophoretic separations and the primary contribution to the band broadening comes from the B term and so the Eq. (10) can be simplified as

$$H_{\text{open}} \approx H_{\text{B}} = \frac{2D_{\text{m}}}{u_{\text{eo,open}}} \tag{11}$$

where D_{m} is the molecular diffusivity of a neutral tracer and $u_{\text{eo,open}}$ is the EOF velocity in the capillary.

For the case of the fully packed column or monolith, the HETP can be calculated as

$$H_{\text{packed}} = H_{\text{A}} + \frac{2D_{\text{m}}}{u^*_{\text{eo, packed}}} + H_{\text{C}} \tag{12}$$

where $u^*_{\text{eo, packed}}$ is the apparent EOF velocity in the column. For most cases, $u_{\text{eo,open}} > u^*_{\text{eo,packed}}$, and so H_{B} is generally higher for the packed columns.

3. Experimental

3.1. Chemicals and reagents

Ethylene glycol dimethacrylate (EGDMA) and polyethyleneimine (PEI, MW 10 000, 30% aqueous) were purchased from Polysciences (Warrington, PA, USA). Vinylbenzyl chloride (VBC) was from Dow (Midland, MI, USA), azobisisobutyronitrile (AIBN) (98%) was from Pfaltz & Bauer (Waterbury, CT, USA) and 3-glycidoxypropyltrimethoxysilane (GPTMS), 3-(trimethoxysilyl)-propyl methacrylate, 2,2-diphenyl-1-picryhydrazyl hydrate (DPPH), trifluoroacetic acid (TFA), succinic acid, toluene, 1-propanol and formamide were from Aldrich (Milwaukee, WI, USA). HPLC reagent-grade sulfuric acid (H_2SO_4), dimethylformamide (DMF) (99%) and analytical-grade hydrochloric acid, monobasic, dibasic and tribasic sodium phosphates and sodium hydroxide (98.8%) were from J.T. Baker (Phillipsburg, NJ, USA). Dimethyl sulfoxide (DMSO) was purchased from Burdick and Jackson (Muskegon, MI, USA). HPLC-grade methanol, acetone, acetonitrile (ACN), and triethylamine were purchased from Fisher (Fair Lawn, NJ, USA). Water was purified and deionized with a NANOpure system (Barnstead, Boston, MA, USA). The individual peptide samples were purchased from Sigma (St. Louis, MO, USA). Single wall carbon nanotubes (SWNT) were synthesized and provided by Yuan Chen, Dr. Dragos Ciuparu and Dr. Lisa D. Pfefferle in the Department of Chemical Engineering at Yale University. The fused silica capillary tubing of 75 μm I.D. × 375 μm O.D. with a polyimide outer coating was purchased from Quadrex Scientific (New Haven, CT, USA).

3.2. Instrumentation

Capillary electrophoresis and capillary electrochromatography experiments were carried out on a HP^{3D}CE capillary electrophoresis unit (Agilent Technologies, Wilmington, DE, USA) equipped with a diode array UV detection system and controlled by a P150 personal computer (Hewlett-Packard, Palo Alto, CA, USA). Windows 95 (Microsoft, Redwood, WA) and Chemstation V.4.01 (Agilent) were installed to control the instrument functions and to process the data. Both inlet and outlet vials were pressurized with nitrogen up to 12.0 bar. The wavelength of the UV detector was set at 214 nm.

3.3. Buffer and mobile phase preparations for HPLC, CE and CEC separations

A stock solution of phosphate buffer (80 mM) was made, and then diluted and adjusted to various concentrations. Before CEC experiments, the running buffer was degassed with helium for about 20 min. The individual peptides were mixed and diluted with deionized water to the appropriate concentration. A 0.01% (v/v) DMSO was prepared with deionized water and used as the unretained neutral marker of EOF in this study.

3.4. Capillary electrophoresis conditions

All experiments were performed at 25 °C with 20 mM phosphate buffer, pH 2.5, as mobile phase. Buffer pH of 2.5 was chosen as for our case, the capillary and the columns are coated with PEI and so do not suffer the instability like fused silica. In fact, we need the low pH for the PEI to be positively charged and generate the EOF. According to the new configuration of the monolithic columns, the experiments were performed isocratically by counter-directional mode with reversed polarity. Between runs, the capillary column was rinsed with deionized water for 3 min, followed with running buffer for 5 min.

Before using, the open bare silica capillary was washed with water and filled with 1.0 M NaOH. With both ends sealed, the tubing was heated at 100 °C for 1 h in the oven of a Sigma 2000 gas chromatograph (Perkin-Elmer, Norwalk, CT, USA). Thereafter, it was washed with deionized water for 10 min, 1.0 M HCl for 5 min, deionized water for 30 min and acetone for 10 min. Subsequently the capillary tubing was placed again in the oven at 120 °C and purged with nitrogen for 1 h to remove residual water [25,26].

For preparation of the GPTMS–PEI coated capillary, an open fused silica capillary was pretreated with NaOH as earlier. Siloxane groups at the inner surface of raw fused silica capillaries were hydrolyzed by NaOH pretreatment to increase the density of silanol groups serving as anchors for the subsequent silanization. Thereafter, the silica capillary was silanized with 10% (v/v) 3-glycidoxypropyltrimethoxysilane with 1% (v/v) triethylamine in dry toluene for 3 h at room

temperature [27–29]. Afterwards, the capillary was flushed with a solution of 7.5% (v/v) polyethyleneimine in 0.05 M succinate buffer (pH 6.0) for 5 h at room temperature [27,30–32].

3.5. Capillary electrochromatography packing and evaluation conditions

All CEC experiments were performed under the same conditions as CE experiments described earlier. Between runs, the capillary column was rinsed with deionized water for 10 min, followed with running buffer for 15 min at 1×10^6 Pa inlet pressure. The column was equilibrated electrokinetically at the operating voltage until the baseline was stable.

The monolithic columns for CEC separation were prepared according to a previously published method [27]. After the silica capillary was coated with GPTMS–PEI as mentioned earlier, a solution containing 20% (v/v) monomer VBC, 20% (v/v) crosslinker EGDMA, 40% (v/v) propanol and 20% (v/v) formamide as porogens, 0.3% AIBN (w/v) as polymerization initiator, was mixed and filled into the column with nitrogen. Subsequently, the capillary column was sealed and heated at 75 °C for 16 h in the oven of a Model Sigma 2000 gas chromatograph (Perkin-Elmer, Norwalk, CT, USA). The capillary was then washed with methanol and deionized water extensively. 10 mM aqueous sodium hydroxide was pumped through the capillary containing the porous poly(VBC–EGDMA) monolith packing at 70 °C for 3 h to hydrolyze the residual benzyl chloride groups at the surface of poly(VBC–EGDMA). After the column was washed with deionized water and methanol, it was purged overnight with nitrogen at room temperature.

The poly(VBC–EGDMA–SWNT) monolithic column with GPTMS–PEI coating was prepared in the similar way using 2-propanol with soluble SWNT as one of the porogens instead of pure propanol. To make them soluble in 2-propanol, SWNT were stirred with a 9:1 98% H_2SO_4/30% H_2O_2 aqueous solution for 30 min and sonicated for 10 min [33]. The resulting SWNT dispersion was diluted and filtered through a 0.45 μm Millipore polycarbonate membrane with distilled water, and was subsequently washed using 10 mM NaOH and distilled water until the pH of the filtrate was 7. The SWNT mat was then separated from the filter by dispersion into 2-propanol, sonicated again and used as one of the porogens in the preparation of the monolithic stationary phase.

To create a detection window, a 1–2 mm wide segment of the polyimide outer coating at a distance of 8.5 cm from the outlet end was heated with an Archer Model B microtorch (Radio Shack, New Haven, CT, USA) while the capillary column was purged with oxygen at 8.3×10^5 Pa. Subsequently, the capillary column was washed with methanol and deionized water.

4. Results and discussion

4.1. Measurement of current

Electrokinetic measurements were performed on the open silica capillary; a coated capillary with GPTMS–PEI coating; monolith 1 with GPTMS–PEI coating and poly(VBC–EGDMA) monolith; and monolith 2 with GPTMS–PEI coating and poly(VBC–EGDMA–SWNT) monolith. Table 1 lists the current and retention time of the tracer measured for these four cases. Measurements were performed in duplicate and averaged for further calculations. It is seen that under the buffer conditions chosen for operation, the EOF is minimal in the bare silica capillary.

Table 2 shows the calculation of the conductivity for the open capillaries and the monoliths using Eqs. (1) and (2), respectively. The conductivity is similar for the bare silica and coated capillaries. This is expected because conductivity is an intrinsic property and is independent of capillary geometry or the potential drop applied [12]. For this case, assuming that we do not have appreciable Joule heating and the EOF itself contributes minimally to the velocity of ions, the conductivity depends only on the buffer used. Since the same buffer is used for measurements on both the open capillaries, the conductivity is also expected to be identical.

The conductivity for the two monolithic columns is lower than that for the open capillaries. This is due to the flow hindrance caused by the monolithic support in the column forcing the ions to follow a more tortuous path through the column. Archie's law in Eq. (3) was used for estimating the

Table 1
Electrokinetic measurements performed on silica capillary, a coated capillary and two monolithic columns

Parameter	Open capillary		Coated capillary		Monolithic column 1		Monolithic column 2	
Total length (cm)	40	40	31	31	40	40	40	40
Detection length (cm)	31.5	31.5	22.5	22.5	31.5	31.5	31.5	31.5
Diameter (μm)	75	75	75	75	75	75	75	75
Voltage (kV)	20	20	20	20	20	20	20	20
Current (μA)	55	56.5	66.1	68.2	21	21.5	24.5	25.2
t_0[a] (min)	>60[b]	>60[b]	2.1	2.26	5.4	5.39	4.19	4.12

Measurements were performed in duplicate with different capillary/column. Open capillary: bare silica; coated capillary: GPTMS–PEI coating; monolith 1: poly(VBC–EGDMA) monolith with GPTMS–PEI coating; monolith 2: poly(VBC–EGDMA–SWNT) with GPTMS–PEI coating. All experiments were performed at 25 °C with 20 mM phosphate buffer, pH 2.5, as mobile phase.

[a] Measurements were made with an inert and neutral marker.

[b] Experiment was stopped after 60 min.

Table 2
Estimation of conductivity, conductivity ratio, and electrokinetic porosity for monolithic columns

Parameter	Open capillary	Coated capillary	Monolithic column 1	Monolithic column 2
σ_{open} (Ω^{-1} m^{-1})	0.25	0.24	N/A[a]	N/A[a]
σ_{packed} (Ω^{-1} m^{-1})	N/A[a]	N/A[a]	0.10	0.11
ϕ	N/A[a]	N/A[a]	0.38	0.45
ε_T	N/A[a]	N/A[a]	0.52	0.58

[a] Not applicable.

Table 3
Comparison of conductivity ratio and electrokinetic porosity of monolithic phases to other commonly used stationary phases

Stationary phase	ϕ	ε_T
Monolithic column 1	0.38	0.52
Monolithic column 2	0.45	0.58
Pellicular Hytach ODS	0.29	0.44
Zorbax ODS, 80 Å	0.28	0.43
Spherisorb ODS, 300 Å	0.49	0.62
Spherisorb SCX, 300 Å	0.52	0.65
Polymer Lab SCX, 1000 Å	0.66	0.76
Bio-Rad SCX	0.67	0.77

Adapted from ref. [17].

electrokinetic porosity, ε_T, for the two monolithic phases. It is seen that monolith 2 is more porous than monolith 1.

Table 3 further compares the monolithic materials to a variety of commonly available stationary phases [17]. Columns packed with larger pore materials offer a more open structure leading to higher conductivity ratios and porosities. It is seen that the two monoliths behave similar to the 300 Å stationary phases with regards to flow of ions.

4.2. Measurement of flow

Table 4 presents calculations of EOF velocity, apparent and actual EOF mobility, equivalent length, and zeta potential for the coated capillary and the two monolithic columns. Eqs. (4)–(9) were used for the calculations using the data presented in Table 1. While the EOF velocity is significantly higher for the case of coated capillary, the apparent mobilities are comparable for the three cases. This is so because the mobility is an intrinsic parameter like conductivity and thus, normalizes for the differences in capillary/column dimensions and other operating parameters. The mobility serves as a useful electrokinetic measure for comparison of different stationary phases. It can be concluded from the data presented in Table 4 that a column containing monolithic phase 2 will generate same EOF as the coated capillary of same dimensions when operated under identical operating conditions.

Equivalent length is calculated for the monolithic columns using Eq. (9). This is an estimation of the actual path traversed by the ions while traveling through porous media [12]. The equivalent length, as seen in Table 4, is much larger than the actual length of the monolithic bed.

Next, the actual EOF mobility in the interstitial space of the column is calculated using Eq. (8). It is seen that the actual mobility for both the monolithic columns is significantly higher than the EOF mobility for the coated open capillary. However, the porous bed structure results in an equivalent apparent EOF mobility for the three cases.

The actual mobility can be used to estimate the zeta potential on the monolithic surface [12,17] and it is seen that the zeta potential is significantly higher than the coated open capillary, particularly for monolith 2. A recent study used a similar approach for estimation and comparison of zeta potential of silica-based anion-exchanger type porous particles including Hypersil and Kromasil stationary phases for CEC [34].

4.3. Measurement of column efficiency

Column efficiency measurements were performed using the tracer peak for the case of coated capillary and the two monolithic columns. Table 5 presents HETP data measured at different voltages. The data shows that the HETP value is significantly higher for monolithic column 1 when compared to the coated open capillary. This is expected for a packed column due to presence of the stationary phase and additional contributions from the flow non-uniformity and mass transfer (H_A and H_C terms in Eq. (10)). However, the HETP values for the monolithic column 2 are quite comparable to that for coated open capillary, particularly at lower potential drops. This indicates that the second monolithic column has a much more uniform flow distribution and enhanced mass transfer.

Table 4
Estimation of EOF velocity, mobility, equivalent length, and zeta potential for the coated capillary and the monolithic columns

Parameter	Coated capillary	Monolithic column 1	Monolithic column 2
EOF velocity ($\times 10^{-3}$ m s^{-1})	1.72	0.97	1.26
Apparent mobility ($\times 10^{-8}$ m^2 s^{-1} V^{-1})	2.67	1.95	2.53
Equivalent length (m)	N/A[a]	64.79	69.75
Actual mobility ($\times 10^{-8}$ m^2 s^{-1} V^{-1})	N/A[a]	3.15	4.41
Zeta potential[b] (mV)	37.71	44.53	62.25

[a] Not applicable.
[b] Values of $\varepsilon = 80$ and $\varepsilon_0 = 8.85$ were assumed for this calculation [12].

Table 5
HETP measurements at different potential drops

Parameter	Coated capillary	Monolithic column 1	Monolithic column 2
Average HETP at 10 kV (μm)	8.47	18.88	9.73
Average HETP at 20 kV (μm)	7.58	23.21	11.27
Average HETP at 30 kV (μm)	13.61	38.90	17.70

Rest of the experimental conditions same as in Table 1.

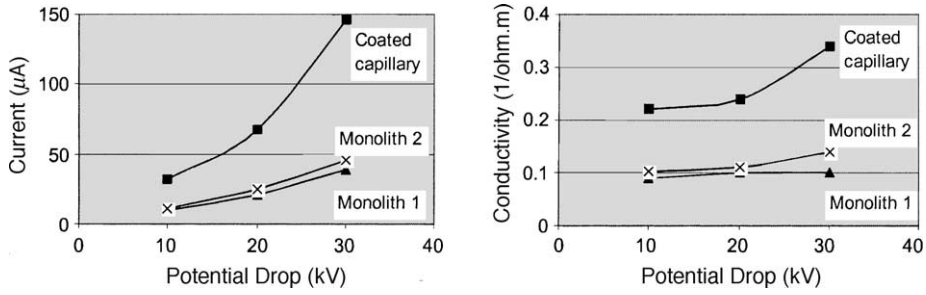

Fig. 1. Plots of current and conductivity vs. potential drop illustrating the extent of Joule heating.

Further, it can be observed in Table 5 that for most cases the HETP increases with the potential drop. Since the measurements were performed with an inert tracer (small H_C) and since the flow velocity is higher at higher potential drop, it follows from Eq. (10) that this trend is a result of Joule heating at higher potential drops. In order to examine the effect of Joule heating, current and conductivity were plotted against the potential drop as shown in Fig. 1. The non-linearity seen in the plots of the current indicate the presence of Joule heating. The final confirmation is presented by the conductivity plots that are expected to be flat in the absence of Joule heating [35]. As seen in Fig. 1, while there is minimal Joule heating in monolith 1 (10% increase over 20 °C), it is significant in monolith 2 (35% increase over 20 °C) and even more so for the coated open capillary (54% increase over 20 °C). We propose that the higher Joule heating and conductivity in monolith 2, compared with monolith 1, were probably due to the unique electronic properties of the incorporated SWNT in the stationary phase, because the SWNT used were reported to show the normal 1:2 distribution between metallic and semiconducting species [36]. It must be pointed out that even though Joule heating can explain the marked increase in HETP with increasing applied voltage for the coated capillary and the monolithic column 2, it is not the reason for the observed increases in HETP for monolithic column 1.

In view of the presence of Joule heating at higher potential drops, further analysis of the different HETP components was performed using data generated at 10 kV. First, the diffusivity was estimated from measurements of the coated open capillary using Eq. (11). Next, the diffusivity value was used to estimate H_B in Eq. (12) and a comparison with the total height equivalent of theoretical plate (HETP) measured for the two monolithic columns allowed us to estimate the $H_A + H_C$ contributions. The results of this analysis are presented in Table 6 and show that for monolith 2, almost all of the HETP can be accounted from longitudinal diffusivity, with minimal contributions from flow non-uniformity (H_A) and/or mass transfer (H_C) contributions. The results for monolith 1 show approximately 30% of the HETP contributions coming from $H_A + H_C$. The analysis allows us to not only estimate the column efficiency, as well as, guide us on possible improvements via changes in media design.

4.4. Separation of peptides

The monolithic columns described earlier have been applied in peptide separations. Four standard peptides including WAGGDASGE, GG, WGG, and GGG had been successfully separated isocratically on both monolith 1 and monolith 2 in the "counter-directional mode". By comparison of the electrochromatograms obtained on both monolithic columns in Fig. 2, it is shown that poly(VBC–EGDMA–SWNT) monolith provided higher speed and efficiency than the corresponding poly(VBC–EGDMA) monolith under the same

Table 6
Estimation of different HETP contributions, H_A, H_B and H_C, for the monolithic columns

Parameter	Coated capillary	Monolithic column 1	Monolithic column 2
Average HETP (μm)	8.47	18.88	9.73
Estimated D_m ($\times 10^{-9}$ m^2 s^{-1})	2.45	N/A[a]	N/A[a]
Estimated H_B (μm)	N/A[a]	12.24	9.69
Estimated $H_A + H_C$ (μm)	N/A[a]	6.64	0.04

Calculations based on HETP measurements of the tracer peak performed at 10 kV. Rest of the experimental conditions same as in Table 1.
[a] Not applicable.

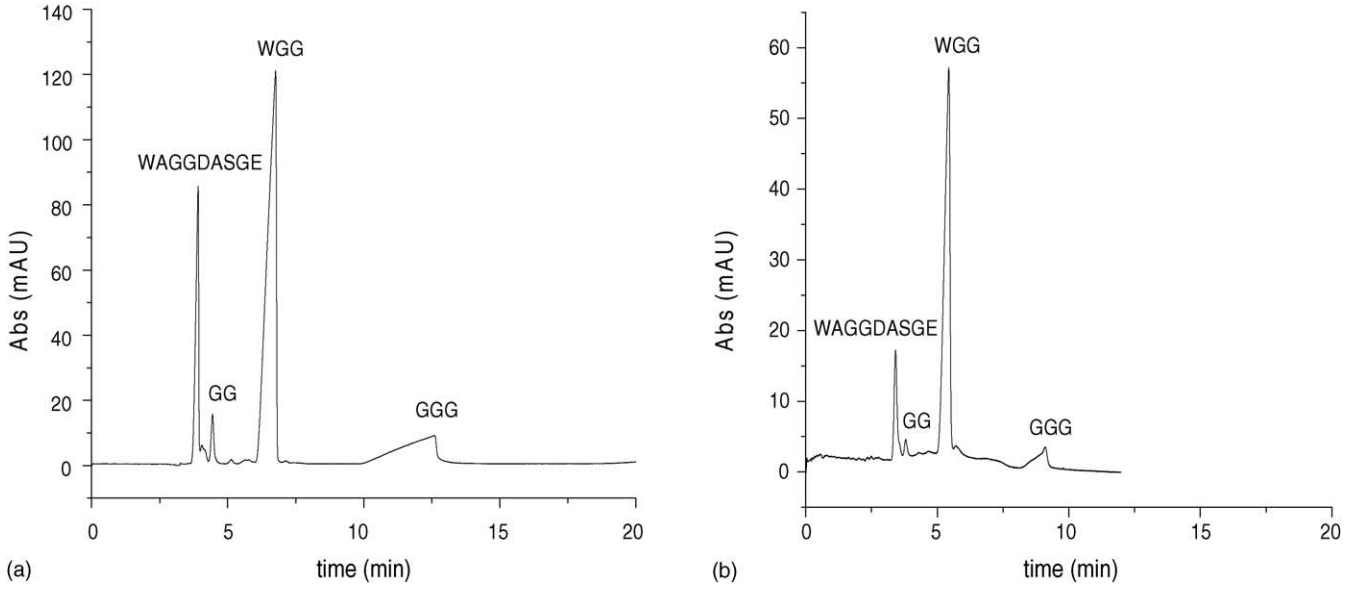

Fig. 2. Electrochromatograms of peptides obtained by CEC with two monolithic columns: (a) monolith 1, 75 μm × 31/22.5 cm, porous poly(VBC–EGDMA) with GPTMS–PEI coating; (b) monolith 2, 75 μm × 31/22.5 cm, porous poly(VBC–EGDMA–SWNT) with GPTMS–PEI coating. Mobile phase, 20 mM aqueous sodium phosphate buffer, pH 2.5 containing 20% (v/v) ACN; applied voltage, 20 kV, reversed polarity; UV detection, 214 nm. Peaks: (1) WAGGDASGE; (2) GG; (3) WGG; (4) GGG.

conditions. It was found that two retained peptides (WAGGDASGE and GG) had the similar efficiencies on monolith 2 as that shown by the inert marker DMSO on both columns. As is shown by our calculations and results presented in Table 6, SWNT incorporated in the monolithic stationary phase 2 offers improved mass transfer and a more uniform flow distribution. The components WGG and GGG elute after the EOF marker illustrating a stronger retention on the stationary phase. For retained components, the mass transfer term tends to dominate the separation efficiency of the system and hence we observe band broadening of WGG and peak fronting of GGG with both monolithic columns. Specific hydrophobic and electrostatic interactions between the particular peptides and the stationary phases may also be occurring here.

Human growth hormone (hGH) tryptic digest was separated by CEC with monolith 2, as shown in Fig. 3. When the hGH tryptic digest sample was injected in Tris buffer, the electrochromatogram showed a large, ill-defined increase in absorbance (Fig. 3a) that was probably due to the mismatch between sample solution and running buffer. As we expected,

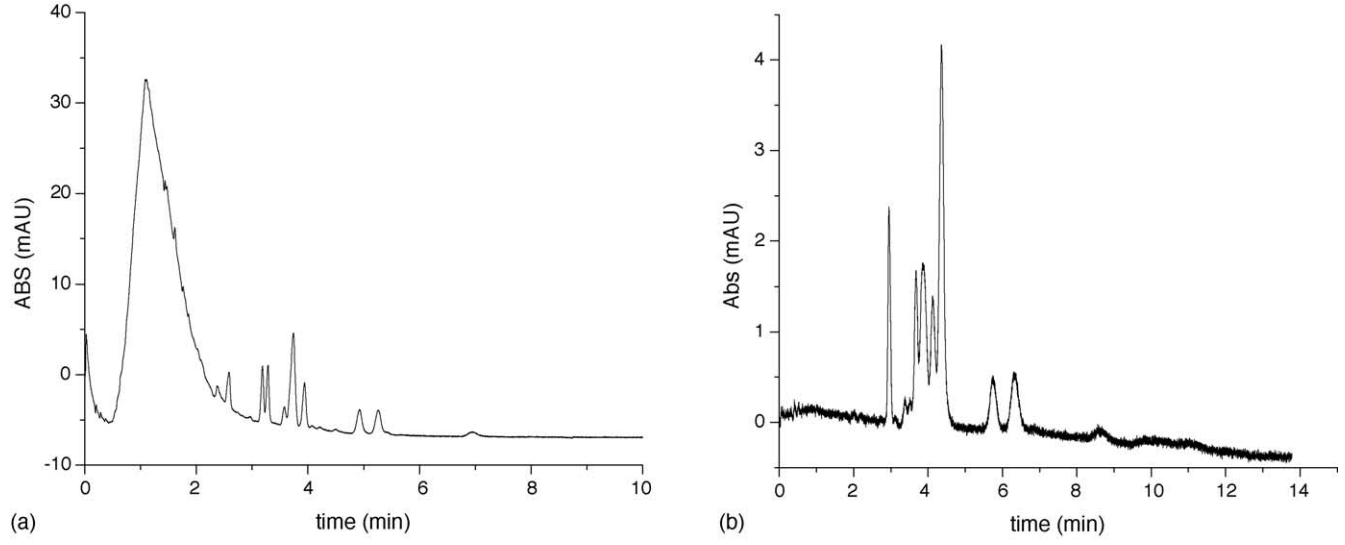

Fig. 3. Electrochromatogram of hGH tryptic digest obtained by CEC with monolith 2: 75 μm × 31/22.5 cm, porous poly(VBC–EGDMA–SWNT) with GPTMS–PEI coating; mobile phase, 20 mM aqueous sodium phosphate buffer, pH 2.5 containing 20% (v/v) ACN; applied voltage, 20 kV, reversed polarity; UV detection, 214 nm. (a) hGH tryptic digest dissolved in Tris buffer; (b) hGH tryptic digest after removing Tris buffer dissolved in running buffer.

a better separation was obtained (Fig. 3b) after Tris buffer was removed from the sample and replaced by the running buffer.

5. Conclusions

An approach for evaluation of the conductivity ratio, porosity, and the interstitial EOF mobility, from experimental data on the current and EOF measured with CEC columns has been presented. It has been shown that this data could be very useful for characterization of the columns and for guiding improvements in column design and materials. It can be concluded that there is a need to distinguish between the apparent and the actual EOF mobilities and to use only the latter for characterizing the various stationary phases. The results of this study are expected to clarify the meaning and significance of the parameters used for characterization of porous media with regard to some electrokinetic phenomena.

Acknowledgements

We are grateful to Yuan Chen, Dr. Dragos Ciuparu and Dr. Lisa D. Pfefferle at Yale University for providing SWNT samples. Part of this work was supported by the National Institute of Health, US Department of Health and Human Services (grant No. GM 20993). This work is dedicated to the memory of our colleague and mentor, Csaba Horváth.

References

[1] M.M. Dittmann, K. Masuch, G.P. Rozing, J. Chromatogr. A 887 (2000) 209.
[2] B. Behnke, E. Bayer, J. Chromatogr. A 680 (1994) 93.
[3] R.J. Boughtflower, T. Underwood, C.J. Paterson, Chromatographia 40 (1995) 329.
[4] A.S. Rathore, Electrophoresis 23 (2002) 3827.
[5] S.E. van de Bosch, S. Heemstra, J.C. Kraak, H. Poppe, J. Chromatogr. A 755 (1996) 165.
[6] K.K. Unger, T. Eimer, Fresenius Z. Anal. Chem. 352 (1995) 649.
[7] A.S. Rathore, Cs. Horváth, J. Chromatogr. A 781 (1997) 185.
[8] L.A. Colon, Y. Guo, A. Fermier, Anal. Chem. 69 (1997) A461.
[9] T. Eimer, K.K. Unger, J. van der Greef, Trends Anal. Chem. 15 (1996) 463.
[10] A.M. Fermier, L.A. Colon, J. Microcolumn Sep. 10 (1998) 439.
[11] W. Wei, G.A. Luo, G.Y. Hua, C. Yan, J. Chromatogr. A 817 (1998) 65.
[12] A.S. Rathore, Cs. Horváth, Anal. Chem. 70 (1998) 3069.
[13] R.E. Majors, LC–GC 16 (1998) 96.
[14] E.C. Peters, M. Petro, F. Svec, J.M.J. Fréchet, Anal. Chem. 70 (1998) 2296.
[15] I.S. Lurie, T.S. Conver, V.L. Ford, Anal. Chem. 70 (1998) 4563.
[16] A.P. McKeown, M.R. Euerby, H. Lomax, J. Sep. Sci. 25 (2002) 1257.
[17] A.S. Rathore, E. Wen, Cs. Horváth, Anal. Chem. 71 (1999) 2633.
[18] G.E. Archie, Trans. AIME 146 (1942) 54.
[19] P. Wong, J. Koplik, J.P. Tomanic, Phys. Rev. B 30 (1984) 6606.
[20] M. von Smoluchowski, in: I. Graetz (Ed.), Handbuch der Elektrizität und des Magnetismus, Barth, Leipzig, 1921, p. 366.
[21] C.L. Rice, R. Whitehead, J. Phys. Chem. 69 (1965) 4017.
[22] J.T.G. Overbeek, in: H.R. Kruyt (Ed.), Colloid Science, Elsevier, New York, 1952, p. 194.
[23] J.J. van Deemter, F.J. Zuiderweg, A. Klinkengberg, Chem. Eng. Sci. 5 (1956) 271.
[24] J.C. Giddings, Unified Separation Science, Wiley–Interscience, New York, 1991.
[25] X. Huang, J. Zhang, Cs. Horváth, J. Chromatogr. A 858 (1999) 91.
[26] J. Zhang, S. Zhang, Cs. Horváth, J. Chromatogr. A 953 (2002) 239.
[27] Y. Li, R. Xiang, Cs. Horváth, J.A. Wilkins, Electrophoresis 25 (2004) 545.
[28] X.W. Shao, Y.F. Shen, K. O'Neill, M.L. Lee, J. Chromatogr. A 830 (1999) 415.
[29] J. Yakovleva, R. Davidsson, A. Lobanova, M. Bengtsson, S. Eremin, T. Laurell, J. Emneus, Anal. Chem. 74 (2002) 2994.
[30] J.K. Towns, F.E. Regnier, J. Chromatogr. 516 (1990) 69.
[31] F.B. Erim, A. Cifuentes, H. Poppe, J.C. Kraak, J. Chromatogr. A 708 (1995) 356.
[32] M.S. Nutku, F.B.E. Berker, Turk. J. Chem. 27 (2003) 9.
[33] W. Zhao, C. Song, P.E. Pehrsson, J. Am. Chem. Soc. 124 (2002) 12418.
[34] O.L. Sánchez Muñoz, E.P. Hernández, M. Lämmerhofer, W. Lindner, E. Kenndler, Electrophoresis 24 (2003) 390.
[35] A.S. Rathore, J. Chromatogr. A 1037 (2004) 431.
[36] T.W. Odom, J.-l. Huang, C.M. Lieber, Ann. N. Y. Acad. Sci. 960 (2002) 203.